

# Structure, reactivity and electronic properties of V-doped Co clusters

Soumendu Datta,<sup>1</sup> Mukul Kabir,<sup>2</sup> Tanusri Saha-Dasgupta,<sup>1</sup> and Abhijit Mookerjee<sup>1,11</sup>

<sup>1</sup>*Department of Material Sciences, S.N. Bose National Centre for Basic Sciences,  
JD Block, Sector-III, Salt Lake City, Kolkata 700 098, India*

<sup>2</sup>*Department of Materials Science and Engineering,  
Massachusetts Institute of Technology, Cambridge, Massachusetts 02139, USA*

(Dated: April 24, 2022)

Structures, physical and chemical properties of V doped  $\text{Co}_{13}$  clusters have been studied in detail using density functional theory based first-principles method. We have found anomalous variation in stability of the doped clusters with increasing V concentration, which has been nicely demonstrated in terms of energetics and electronic properties of the clusters. Our study explains the nonmonotonic variation in reactivity of  $\text{Co}_{13-m}\text{V}_m$  clusters towards  $\text{H}_2$  molecules as reported experimentally [J. Phys. Chem. **94**, 2744 (1990)]. Moreover, it provides useful insight into the cluster geometry and chemically active sites on the cluster surface, which can help to design better catalytic processes.

## I. INTRODUCTION

The interest in the studies of clusters is largely because of their possible technological applications which include the possibilities of developing novel cluster-based materials using the size dependence of their properties. Doping of clusters is an important possibility in this direction. In recent times the fabrication of alloy clusters of different sizes with well defined, controlled properties by varying the composition and atomic ordering, has caught considerable attention.<sup>1,2</sup> Bimetallic alloy clusters have been known and exploited for last few years in various applications, specially in the catalytic reactions.<sup>3,4</sup> Varying the ratio of the two constituents, one can alter the surface structures, compositions and segregation properties.<sup>5,6</sup> In this way, it is possible to tune the chemical reactivity at the surface of an alloyed cluster.<sup>7,8</sup> Considering the huge possibility of using nano clusters in catalysis, the study of cluster reactivity has become an interdisciplinary topic of present day research.<sup>9,10,11,12</sup>

About two decades ago, Nonose *et al* measured the reactivity towards  $\text{H}_2$  of bimetallic  $\text{Co}_n\text{V}_m$  ( $n > m$ ) clusters using laser vaporization technique and reported strong cluster size and composition dependence.<sup>13</sup> Both V and Co are  $3d$  transition metals. The substitution of Co by V atoms, one by one, should increase the reactivity of the alloy cluster towards  $\text{H}_2$  molecules, as V, an early transition metal, has a high reactivity towards  $\text{H}_2$  in contrast to Co which has relatively low reactivity.<sup>14</sup> Interestingly, it was found that the reactivity increased gradually, as expected, with the substitution of Co atom by V atom one by one in the  $\text{Co}_n$  clusters ( $n < 13$ ), but for the  $\text{Co}_{13}$ , there was a remarkable decrease in reactivity when a single Co atom was substituted by a V atom. However, the reactivity increased as the number of exchange V-atoms increased further up to  $m = 3$ , while the fourth V-atom substitution did not increase the reactivity any more. In view of the high reactivity of elemental V, this sudden drop in reactivity of the  $\text{Co}_{12}\text{V}$  cluster was rather surprising. The authors speculated a plausible icosahedral structure for the  $\text{Co}_{12}\text{V}$  cluster with the active V atom

at the cage center. Therefore, the V atom, being shielded geometrically from  $\text{H}_2$  by the twelve surface Co atoms, might have less chance to interact with H-atoms. The chemisorption reactivity of cationic  $\text{Co}_{13-m}\text{V}_m^+$  clusters<sup>15</sup> and anionic  $\text{Co}_{13-m}\text{V}_m^-$  clusters<sup>16</sup> also shows similar type of variation as that of neutral  $\text{Co}_{13-m}\text{V}_m$  clusters, which hints towards the dominant effect of geometric structure as compared to the electronic structure. For clusters, the ionization potential (IP) depends on the position of the highest occupied molecular orbital (HOMO) level. For the pure metal clusters, Whetten *et al* have postulated that the reaction rate for cluster- $\text{H}_2$  dissociative chemisorption is determined by the charge transfer from the HOMO to the lowest unoccupied molecular orbital (LUMO) of the reactant gas  $\text{H}_2$ , and an anti-correlation between IP and reaction coefficient could be observed.<sup>17</sup> That means lower value of IP corresponds to higher reactivity and vice versa. However, the ionization energies of the  $\text{Co}_n\text{V}_m$  clusters, measured by Hoshino *et al* using photo-ionization spectroscopy show no such anti-correlation,<sup>18</sup> again demonstrating the importance of geometrical structure. A rigorous first-principles study in terms of geometric and electronic effects is therefore very much needed to understand this anomalous nature of reactivity of  $\text{Co}_{13-m}\text{V}_m$  ( $m = 0-4$ ) clusters. In this report, we have carried out an *ab-initio* theoretical study on V doped  $\text{Co}_{13}$  clusters. The whole study can be divided into three major parts : first part consists of an exhaustive search for the minimum energy structures (MES) for cluster of each composition, followed by stability analysis of these MES in terms of various physical quantities in the second part, while the final part includes investigation of chemisorbed structures and understanding of cluster reactivity.

## II. COMPUTATIONAL DETAILS

The calculations have been performed using density functional theory (DFT), within the pseudopotential plane wave method as implemented in VASP code.<sup>19</sup> We have used the projector aug-

mented wave (PAW) pseudopotentials<sup>20,21</sup> and the Perdew-Bruke-Ernzerhof (PBE) exchange-correlation functional<sup>22</sup> for spin-polarized generalized gradient approximation (GGA). The 3*d* and 4*s* electrons were treated as the valence electrons for the transition metal elements and the wave functions were expanded in the plane wave basis set with the kinetic energy cut-off of 335 eV. The convergence of the cluster energies with respect to the cut-off value has been checked. Reciprocal space integrations were carried out at the  $\Gamma$  point. Symmetry unrestricted geometry and spin optimizations were performed using the conjugate gradient and the quasi-Newtonian methods until all the force components were less than a threshold value of 0.005 eV/Å. In order to ensure the structural trends found in the optimized structures, we have also carried out Bohn-Openheimer molecular dynamics<sup>23</sup> within LDA for few specific clusters. Simple cubic super-cells were used for cluster calculations with the periodic boundary conditions, where two neighboring clusters were kept separated by at least 12 Å vacuum space to make the interaction between the cluster images negligible. The cohesive energy ( $E_c$ ) of a  $\text{Co}_n\text{V}_m$  alloy cluster is calculated with respect to the free atoms as

$$E_c(\text{Co}_n\text{V}_m) = mE(\text{V}) + nE(\text{Co}) - E(\text{Co}_n\text{V}_m) \quad (1)$$

where  $E(\text{Co}_n\text{V}_m)$ ,  $E(\text{Co})$  and  $E(\text{V})$  are the total energies of  $\text{Co}_n\text{V}_m$  cluster, an isolated Co atom and an isolated V atom respectively. One can also define the cohesive energy with respect to the Co and V bulk phases at equilibrium instead of isolated atoms. However, the cohesive energy variation with increasing V-concentration follows the same trend irrespective of the way of cohesive energy definition. The second difference in energy for fixed size ( $n + m = \text{constant}$ ) and variable composition is defined as

$$\Delta_2 E(\text{Co}_n\text{V}_m) = E(\text{Co}_{n+1}\text{V}_{m-1}) + E(\text{Co}_{n-1}\text{V}_{m+1}) - 2E(\text{Co}_n\text{V}_m) \quad (2)$$

It gives the relative stability of alloy clusters having nearby compositions.

### III. STRUCTURE

Since chemical reaction with clusters takes place on its surface, the atomic arrangement and the composition of cluster surface play an important role in chemical reactivity. Therefore, the first step towards the theoretical modeling of clusters is to determine their ground state structure. In our earlier work,<sup>24</sup> we studied the structure and magnetism of the pure Co clusters in detail. To obtain the MES having the optimized geometry as well as the optimized magnetic moment, we considered several probable starting geometries having closed packed atomic arrangement and allowed each of the geometries to relax for *all possible* collinear spin configurations of the

atoms. We follow the same way of structural optimization here for the V doped Co clusters ( $\text{Co}_{13-m}\text{V}_m$ ;  $m = 1-4$ ). However, the situation for alloy clusters is quite cumbersome as one has to deal with a large number of starting geometries because of the presence of *homotops* (the term was first coined by Jellinek<sup>25,26</sup>). The *homotops* have the same number of atoms, composition and geometrical structure, but differ in the arrangement of the doped atoms. As for example, a single geometrical structure of an  $\text{A}_n\text{B}_m$  alloy cluster with fixed number of atoms ( $N = m + n$ ) and composition ( $m/n$  ratio), will give, in principle,  $\frac{N!}{m!n!}$  *homotops*. Some of them, however, may be symmetry equivalent and the number of the inequivalent *homotops* will be somewhat less than the above mentioned value. So the variety of structures in alloy clusters is much richer than that of the pure clusters and the potential energy surface of even a small cluster of few tens of atoms is of enormous complexity.

It is generally found that the transition metal clusters prefer compact geometries to maximize the interaction between the rather localized *d* orbitals.<sup>27</sup> There are three most compact and highly coordinated structures for 13 atoms cluster: icosahedron, cub-octahedron and hexagonal closed packed (HCP) geometries. We have therefore considered these three geometries as the most probable starting structures. For the pure  $\text{Co}_{13}$  cluster, we found that the MES is a distorted HCP geometry with total magnetic moment of 25  $\mu_B$  and total cohesive energy of 42.63 eV as mentioned in our previous work.<sup>24</sup> The structure has 22 triangular faces and 33 edges (cf. Fig. 1). This hexagonal growth of the pure Co clusters is quite unusual compared to the trend seen in the clusters of its 3*d* neighbors like Mn, Fe, Ni, which preferably adapt an icosahedral pattern.<sup>28,29,30</sup> Further study is needed to explore the unusual structural pattern of small pure Co clusters.<sup>31,32</sup> Another distorted structure of HCP motif with total magnetic moment of 27  $\mu_B$  and 0.14 eV above the minimum energy state, is the first isomer. The optimal icosahedral structure of total spin 31  $\mu_B$  (structure having 20 triangular faces and 30 edges) is 0.17 eV higher than the minimum energy state and emerges as the second isomer. The third isomer is a distorted cub-octahedron with total magnetic moment 25  $\mu_B$  and it is 0.22 eV above the minimum energy state. The structures of the ground state, second and third isomers are shown in Fig. 1. It is to be noted that for the pure  $\text{Co}_{13}$  cluster, all the atomic moments are ferromagnetically coupled and our predicted magnetic moment of the ground state structure is in good agreement with the experimental value which is 2.0  $\mu_B/\text{atom}$ .<sup>33</sup>

In the case of single V atom doped  $\text{Co}_{12}\text{V}$  clusters, we have again considered the starting geometries of icosahedral, HCP and cub-octahedral symmetries. However, depending upon the position of the singly doped V-atom either at the center or on the surface, it can give rise to several *homotops*. Again, the surface atoms of a 13-atoms cluster are not equivalent in terms of number of neighbors and their relative positions in case of HCP and

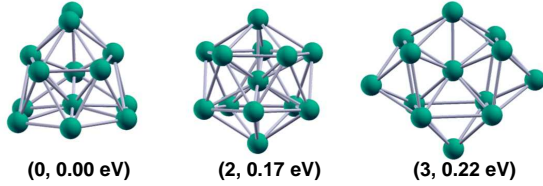


FIG. 1: (Color online) Structures of optimal HCP, icosahedron and cub-octahedron of pure  $\text{Co}_{13}$  cluster (from left to right respectively). The first entry in the parenthesis gives the isomeric position (“0” means minimum energy state) and the second entry corresponds to relative energy to the minimum energy state.

cuboctahedral structures, while for icosahedral structure, all the surface atoms are equivalent. This consideration will give few more starting geometries. So we have considered all these possible geometrical structures and for each of them, we have considered the *all possible* collinear spin alignments during relaxation. Upon optimization of geometry and spin degrees of freedom, we find that an icosahedral structure of total magnetic moment  $25 \mu_B$ , with V atom doped at the center position, is the MES. Now there are several interesting points to note in the context of the  $\text{Co}_{12}\text{V}$  cluster. First of all, the cohesive energy of the MES is considerably higher (by 1.29 eV) than that of the pure  $\text{Co}_{13}$  clusters, indicating its exceptional stability. Secondly, the V doped Co-clusters are found to prefer the icosahedral growth pattern, instead of HCP growth pattern, as we observed in case of the pure Co-clusters. Therefore, just the single V-atom doping in  $\text{Co}_{13}$  changes the equilibrium structure from HCP to icosahedron. This HCP to icosahedron structural transition has also been reported previously for Mn doping in  $\text{Co}_{13}$  cluster.<sup>34</sup> Finally, the single V-atom likes to fit at the center of the icosahedron and it is ferrimagnetically coupled with the surface Co-atoms. The first isomer is also a central V-atom doped icosahedral  $\text{Co}_{12}\text{V}$  cluster, with total magnetic moment  $23 \mu_B$  and it is about 0.46 eV above the MES. Center V doped cub-octahedral  $\text{Co}_{12}\text{V}$  cluster with  $23 \mu_B$  magnetic moment which has energy 0.70 eV higher than the minimum energy icosahedral structure, is the second isomer. The third isomer is a center V doped icosahedron with total magnetic moment of  $27 \mu_B$ . Center V doping in case of HCP cluster is less favorable and appears as the fifth isomer in our calculation with total magnetic moment  $25 \mu_B$  and energy 0.80 eV above the MES. We have also considered the optimal structure of  $\text{Co}_{13}$  (distorted HCP) as the starting structure and substituted the most coordinated central Co-atom by a V-atom. After relaxation considering *all possible* spin alignments, it is found that the shape of the optimal structure remains more or less same as that of the optimal HCP  $\text{Co}_{13}$  cluster and energetically, it is the fourth isomer with total magnetic moment  $23 \mu_B$ . The most probable surface V-doping has a cub-octahedral structure with total magnetic mo-

ment  $21 \mu_B$ , but it is about 1.32 eV above the MES. The structure of ground state and few isomers for the  $\text{Co}_{12}\text{V}$  cluster are shown in Fig. 2.

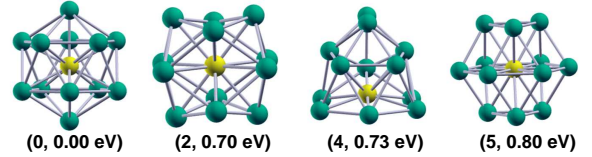


FIG. 2: (Color online) Structures of optimal icosahedron, optimal cub-octahedron and two HCP geometries (from left to right) for  $\text{Co}_{12}\text{V}$  cluster. Green dot represents Co atom, while yellow dot represents V-atom. The entries in the parenthesis have same meaning as in Fig. 1.

Because of the icosahedral growth preference of the  $\text{Co}_{12}\text{V}$  cluster and the presence of the singly doped V-atom at the central site, we consider only the icosahedral symmetry based geometries as the starting guess for more than one V atom doped clusters, in which one V atom is always at the center position, while the residual V atoms reside on the surface. For  $\text{Co}_{11}\text{V}_2$  cluster, the second V atom can replace any of the surface Co atoms, as all the surface sites of a 13-atom icosahedron, are equivalent. After relaxation for *all possible* spin configurations, we find that the MES has total magnetic moment of  $19 \mu_B$  and total cohesive energy of 43.22 eV. The first and second isomers have magnetic moments of  $21 \mu_B$  and  $17 \mu_B$  and they are 0.10 eV and 0.25 eV above the minimum energy state respectively. In the MES, the center V-atom is again ferrimagnetically coupled with the surface Co atoms and has much lower local magnetic moment as it was in the case of the  $\text{Co}_{12}\text{V}$  cluster, while the surface V atom has the maximum local magnetic moment and it is also ferrimagnetically coupled with the other surface Co atoms.

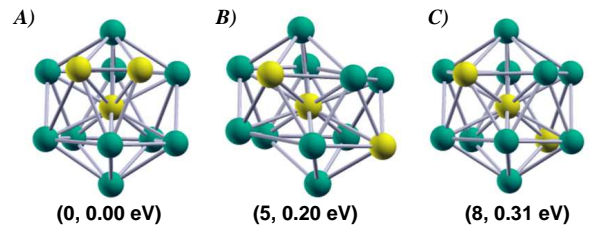


FIG. 3: (Color online) A, B, C represent the three inequivalent *homotops* in icosahedral  $\text{Co}_{10}\text{V}_3$  structure having one V-atom always at the center. The three structures are the optimal structures for the respective three types. The entries in the parenthesis have same meaning as in Fig. 1. Color convention for atoms is same as in Fig. 2.

For  $\text{Co}_{10}\text{V}_3$  cluster, depending upon the different positions of the two surface V atoms, there are three possible icosahedral structures as shown in Fig. 3. However, the structure of type A where the two surface V atoms

are closest to each other, appears as the most favorable one. This type *A* icosahedral structure with total magnetic moment of  $21 \mu_B$  is the minimum energy state with ferrimagnetic alignment of the central V-atom and ferromagnetic alignment of the surface V-atoms with the surface Co-atoms. Both the central and the surface V-atoms have small values of local magnetic moments in this case. There are several closely spaced isomers of type *A* icosahedron with magnetic moments of  $19 \mu_B$ ,  $13 \mu_B$ ,  $23 \mu_B$  and  $17 \mu_B$  which are just 0.04 eV, 0.08 eV, 0.09 eV and 0.15 eV above the MES. We find that the optimal structures of type *B* and type *C* are 0.20 eV and 0.31 eV above the MES, respectively and both of them have same total magnetic moment of  $13 \mu_B$ .

For  $\text{Co}_9\text{V}_4$ , there are three V atoms on the surface. Considering two surface V atoms at closest to each other (following the ground state configuration of  $\text{Co}_{10}\text{V}_3$ ), different positions of the third surface V atom can give rise to the four icosahedral configurations as shown in Fig. 4. After optimization, it is found that the type *A* is the most favorable structure where all the three surface V atoms are closest to each other and form an octahedron with the central V atom. The optimal structure of type *A* icosahedron has total magnetic moment of  $15 \mu_B$  and total cohesive energy of 42.35 eV. Another type *A* icosahedrons with magnetic moments of  $13 \mu_B$ ,  $19 \mu_B$ ,  $21 \mu_B$  and  $17 \mu_B$  are just 0.03 eV, 0.07 eV, 0.09 eV and 0.13 eV above the MES. The optimal type *B*, type *C* and type *D* icosahedrons have total magnetic moments of  $15 \mu_B$ ,  $13 \mu_B$  and  $15 \mu_B$  respectively and they are 0.15 eV, 0.25 eV and 0.33 eV above the MES.

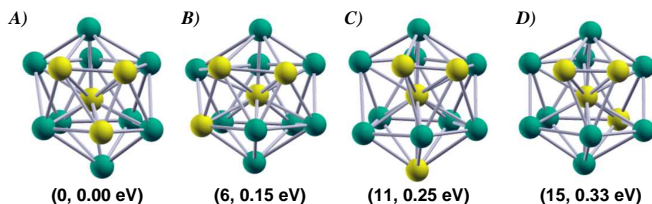


FIG. 4: (Color online) *A*, *B*, *C*, *D* represent the four probable *homotops* in icosahedral  $\text{Co}_9\text{V}_4$  structure having one V-atom at the center and two of the remaining three V-atoms are closest to each other on the surface, while the position of the fourth V-atom is varied. The four structures represented above are the optimal structures for the respective four types. The entries in the parenthesis have same meaning as in Fig. 1. Color convention for atoms is same as in Fig. 2.

The results of the structural optimizations, therefore, can be summarized as, unlike an HCP growth pattern of the pure Co cluster, the V doped  $\text{Co}_{13}$  clusters prefer to adopt an icosahedral packing. In such clusters, the most coordinated central site is occupied by a V-atom, while the residual V-atoms sit on the surface. The surface V-atoms like to be closer to each other to form a group, thereby imparting more distortion to the structure and significantly alter the local surface charge density. The central V-site in the MES of all compositions, is always

ferrimagnetically coupled and has lower magnetic moment. On the other hand, the surface V-atoms can be ferrimagnetically or ferromagnetically coupled with the surface Co-atoms and their local magnetic moments can be as low as the central V-site or as high as the surface Co-site, depending upon the distribution of surface charge density in the clusters having different amount of V-doping. Our prediction of icosahedral geometry for the minimum energy states of V doped Co clusters is in accordance with the speculation of a closed shell geometry around the central site in Ref. 13 and Ref. 15.

To have more confidence about the structural trend as observed above, we have carried out few *ab-initio* molecular dynamics (MD) study for the  $\text{Co}_{12}\text{V}$  and  $\text{Co}_{10}\text{V}_3$  clusters. To determine the lowest energy structures, we have heated up the clusters to 2000 K (which is close to the melting temperature 1768 K for bulk Co and 2183 K for bulk V). The clusters have then been maintained at this temperature for at least 6 ps and then allowed to cool again to 0 K. The cooling process has been done for 24 ps and maintained a very slow cooling rate of 1 K per one iteration throughout the process. The main results obtained from the MD run are : (a) it prefers to adopt the icosahedral pattern with same magnetic alignment of atoms as we predicted from zero temperature relaxation, (b) For the  $\text{Co}_{12}\text{V}$  cluster, the V atom occupies the central position, (c) the surface V atoms for the  $\text{Co}_{10}\text{V}_3$  cluster, prefer to be closest to each other. These results provide reassurance and more confidence in our zero temperature relaxation.

## IV. STABILITY ANALYSIS

The observed atomic arrangement of the MES of the  $\text{Co}_{13-m}\text{V}_m$  clusters as described in the previous section depends critically on the balance of several parameters like the relative strengths of various kinds of bonds present in a cluster structure, the relative atomic sizes, the amount of charge transfer between two different species of atoms, the energy gap between the HOMO and the LUMO, abundance of states near Fermi energy etc. Below, we try to understand the structural stability of the clusters in terms of these parameters.

### A. Cohesive energy

Fig. 5 shows the plot of the cohesive energies of the MES of the  $\text{Co}_{13-m}\text{V}_m$  clusters with increasing V concentration. The plot is with respect to the cohesive energy of the MES of  $\text{Co}_{13}$  cluster. It is seen that the binding has increased considerably compared to that of the optimal  $\text{Co}_{13}$  cluster with single V atom doping. However, the cohesive energies decrease sharply for the higher concentration of V-atoms. For the double and triple V-atom doping, the cohesive energies are above the dashed line indicating their higher stability compared to the pure

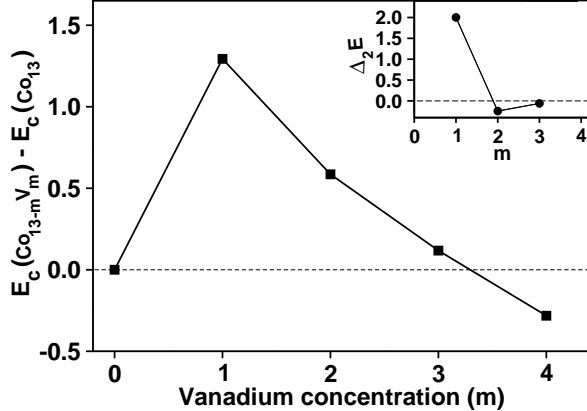


FIG. 5: Cohesive energy of the minimum energy structures of  $\text{Co}_{13-m}\text{V}_m$  clusters with respect to the cohesive energy of minimum energy pure  $\text{Co}_{13}$  cluster. The dashed line is the reference fixed at the cohesive energy of pure  $\text{Co}_{13}$ . Inset shows the second difference ( $\Delta_2 E$ ) in cohesive energy [as defined in Eqn. (2)] for  $\text{Co}_{12}\text{V}$ ,  $\text{Co}_{11}\text{V}_2$  and  $\text{Co}_{10}\text{V}_3$ .

$\text{Co}_{13}$ , while for the fourth V-atom doping, the cohesive energy is even lower than that of the pure  $\text{Co}_{13}$ . The relative stability among the clusters of nearby concentrations is more distinct when we plot the second difference in cohesive energies in the inset of Fig. 5. We use Eqn. 2 to calculate the second difference. A sharp pick in the  $\Delta_2 E$  at  $m = 1$  points to the exceptional stability of the single V-doped cluster compared to the undoped or more than one V-doped clusters.

In order to understand the stability of the doped clusters, we have calculated the cohesive energies and the bond lengths of the Co-Co, Co-V and V-V dimers as shown in Table I. It is seen that the  $\text{V}_2$  dimer is the most stable and the bond length of the  $\text{V}_2$  dimer is also about 14% shorter than that of the  $\text{Co}_2$  dimer which has the least binding among the three. On the other hand, the cohesive energy and bond length of the Co-V dimer are intermediate of the  $\text{Co}_2$  and the  $\text{V}_2$  dimers. For the  $\text{Co}_{12}\text{V}$  cluster, we have seen that the center doping in icosahedral structure is the most favorable. Binary clusters are known to have the problem of segregation, where the doped atom can segregate at the surface or center. To a first approximation, if one of the homonuclear bonds is the strongest, then that species tends to be at the center of the cluster.<sup>1</sup> Our finding of central V-doping is in accordance with this, as the  $\text{V}_2$  dimer has the strongest binding. The atomic radius of a Co-atom and a V-atom, being almost same, the substitution of the central Co atom in an icosahedral  $\text{Co}_{13}$  cluster by a V atom leaves the structure almost unperturbed. As for evidence, the center to vertex average distance and the average distance between two nearby vertices in the opti-

TABLE I: Cohesive energies and bond lengths of  $\text{Co}_2$ , Co-V and  $\text{V}_2$  dimers in the present calculation. For comparison, we have also listed the experimental values for  $\text{Co}_2$  dimer (Ref. 35) and  $\text{V}_2$  dimer (Ref. 36).

Dimer	Cohesive energy (eV/atom)		Bond length ( $\text{\AA}$ )	
	Theory	Expt.	Theory	Expt.
$\text{Co}_2$	1.45	1.72	1.96	2.31
CoV	1.53	...	1.87	...
$\text{V}_2$	1.81	2.47	1.72	1.77

mal icosahedral structure of the  $\text{Co}_{13}$  cluster are 2.334  $\text{\AA}$  and 2.450  $\text{\AA}$ . For the optimal  $\text{Co}_{12}\text{V}$  cluster, these values are almost same, 2.344 and 2.465  $\text{\AA}$  respectively. Therefore the large gain in cohesive energy of the  $\text{Co}_{12}\text{V}$  cluster over that of the  $\text{Co}_{13}$  cluster may be due to the enhanced cohesive energy of the CoV dimer over that of the  $\text{Co}_2$  dimer, though an atom in a dimer is quite different from an atom at the center of a 13-atom cluster. The V atom being at the central position, there are maximum number of CoV dimers in V-doped clusters.

For the clusters doped with more than one V atom, the favorable structure is again found to be of an icosahedral motif, in which the central site is always possessed by a V-atom and the other V-atoms lie on the surface. The number of the surface V atoms and the V-V bonds, therefore, increases with increasing V doping. It favors better binding. On the other hand, the presence of the V-atoms on the cluster surface distorts the cluster geometry and increases the center to vertex average distance as well as the vertex-vertex average distance. Effectively, the cluster volume increases with the increasing V-concentration, which destabilizes the structure. In Table II, we have listed the average distances between center to vertex as well as between two nearby vertices for the MES of  $\text{Co}_{13-m}\text{V}_m$  ( $m = 0-4$ ). We believe that the distortion in the structures is due to the charge density variation induced by the presence of the V-atoms on the cluster surface. The strained cluster structures resulted from distortion can be realized from some open bonds in Fig. 3 and Fig. 4. Therefore, though the number of the V-V bonds increases, which has better binding compared to the Co-Co or Co-V bonds, the overall cohesive energy decreases monotonically as we go from  $\text{Co}_{12}\text{V}$  to  $\text{Co}_9\text{V}_4$  by successive doping of V-atoms. It is then obvious that the cluster geometry and the distribution of atoms on the cluster surface play an important role in deciding the cluster stability.

At this point, it is interesting to study the structure and energetics of the pure  $\text{V}_{13}$  cluster. Since experiment hints symmetric structure for the  $\text{V}_{13}$  cluster<sup>37</sup>, we considered an icosahedral geometry and optimized it considering *all possible* spin configurations. Interestingly, the decreasing trend of cohesive energies for the  $\text{Co}_{13-m}\text{V}_m$  clusters with increasing V-concentration continues also

TABLE II: The average distances in Å between center to vertex and between two nearby vertices for the minimum energy structures of all the studied clusters. For Co<sub>13</sub>, the values correspond to the optimal icosahedron.

Bonds	Co <sub>13</sub>	Co <sub>12</sub> V	Co <sub>11</sub> V <sub>2</sub>	Co <sub>10</sub> V <sub>3</sub>	Co <sub>9</sub> V <sub>4</sub>
center-vertex	2.334	2.344	2.354	2.375	2.398
vertex-vertex	2.455	2.465	2.476	2.499	2.509

at  $m = 13$  *i.e.* pure V<sub>13</sub> cluster. The cohesive energy of the optimal V<sub>13</sub> cluster is found to be lower than that of the pure Co<sub>13</sub> cluster by about 3.73 eV. It indicates that V<sub>13</sub> would be more reactive than any of the V-doped Co<sub>13</sub> clusters. This tendency may be rationalized by considering the case of bulk V and Co, where the bulk V is more reactive than Co because of the lower  $d$ -band filling, relatively higher position of  $d$ -band center and larger  $d$ -band width of V compared to Co. However, pure V does not have importance in catalysis because its high reaction tendency with absorbate tends to poison the surface, without leaving any active site. The desorption energy is also high because of strong V-absorbate bond, which is again not favorable for catalysis.

### B. Spin gap

Analogous to HOMO-LUMO gap of a nonmagnetic cluster, one can define spin gaps for a magnetic cluster as,

$$\begin{aligned}\delta_1 &= - \left[ \epsilon_{\text{HOMO}}^{\text{majority}} - \epsilon_{\text{LUMO}}^{\text{minority}} \right] \\ \delta_2 &= - \left[ \epsilon_{\text{HOMO}}^{\text{minority}} - \epsilon_{\text{LUMO}}^{\text{majority}} \right]\end{aligned}\quad (3)$$

and the system is said to be stable if both  $\delta_1$  and  $\delta_2$  are positive *i.e.* the LUMO of the majority spin lies above the HOMO of the minority spin and vice versa. These represent the energy required to move an infinitesimal amount of charge from the HOMO of one spin channel to the LUMO of the other. So magnitude of spin gaps is a measure of chemical activeness of clusters. Higher gap means less reactive and vice versa. The positions of the HOMO and LUMO in both the spin channels and the values of  $\delta_1$  and  $\delta_2$  for the optimized structures of 13-atom V-doped Co clusters of all compositions considered here are given in Table III.

It is seen that both the spin gaps  $\delta_1$  and  $\delta_2$  are positive for all the clusters. Also Co<sub>12</sub>V has the maximum value of  $\delta$ 's which again indicates the highest stability of Co<sub>12</sub>V cluster compared to the others. Because of this large spin gap, Co<sub>12</sub>V has very low reaction tendency towards H<sub>2</sub> molecules. However, gap values decrease with increasing V concentration and therefore reactivity also increases as observed experimentally.<sup>13</sup>

TABLE III: Positions of HOMO and LUMO in both the spin channels and the values of  $\delta_1$  and  $\delta_2$  for the optimized structures of all compositions.

Cluster	Majority channel		Minority channel		Spin gap (eV)	
	HOMO	LUMO	HOMO	LUMO	$\delta_1$	$\delta_2$
Co <sub>13</sub>	-3.60	-3.35	-3.48	-3.34	0.26	0.13
Co <sub>12</sub> V	-3.93	-2.61	-3.39	-3.34	0.59	0.78
Co <sub>11</sub> V <sub>2</sub>	-3.71	-2.83	-3.43	-3.32	0.39	0.60
Co <sub>10</sub> V <sub>3</sub>	-3.41	-2.98	-3.34	-3.26	0.15	0.36
Co <sub>9</sub> V <sub>4</sub>	-3.46	-3.02	-3.33	-3.17	0.29	0.31

### C. Density of states (DOS)

Fig. 6 shows the spin-polarized total DOS, Co projected DOS, V-projected DOS and total  $d$ -orbital projected DOS for the MES of Co<sub>12</sub>V, Co<sub>11</sub>V<sub>2</sub>, Co<sub>10</sub>V<sub>3</sub> and Co<sub>9</sub>V<sub>4</sub> clusters. It is seen that the total DOS and the total  $d$ -projected DOS are almost overlapping each other. This indicates that the cluster properties are mostly dominated by the  $d$ -electrons which is generally expected for transition metal clusters. The trend in structural stability and reactivity of the clusters as discussed in the previous sections, is also obvious from the nature of the total DOS. The majority spin channel of each cluster has a gap. This gap is maximum for the Co<sub>12</sub>V cluster and it decreases as the number of surface V-atoms increases. In the minority spin channel, there is finite amount of states at the Fermi energy and these are contributed solely by the exterior surface atoms, as the central atom does not have any contribution at the Fermi energy (cf. Fig. 7). It is also seen that the states are more localized in case of the Co<sub>12</sub>V cluster, while they are gradually spreading out and therefore the DOS height, specially in the majority spin channel, decreases with the increasing V-concentration. At this point it is relevant to mention a common feature observed in case of extended surface. The gaseous molecules absorb well on clean surface of an early transition metal as well as on the surface with a multilayer of late transition metal, but not on the surface with a monolayer of late transition metal. For example, the photoemission experiments by El-Batanouny *et al.*<sup>38</sup> showed that a H atom adsorbs well both on the clean Nb(110) surface as well as on the surface with a multilayer of Pd, but does not adsorb on Nb(110) surface with a monolayer of Pd and this is due to the decrease of density of states of  $d$ -electrons of Pd near the Fermi level. Similar behavior had been observed also in case of a monolayer of Pd on W(110) surface, in the experiment of CO-adsorption.<sup>39</sup> Although, a cluster of 13 atoms is substantially different in its property from that of the surface or bulk, one may resemble the stability of the Co<sub>12</sub>V cluster towards H-adsorption with that of extended surface, where the central V atom of Co<sub>12</sub>V corresponds to an

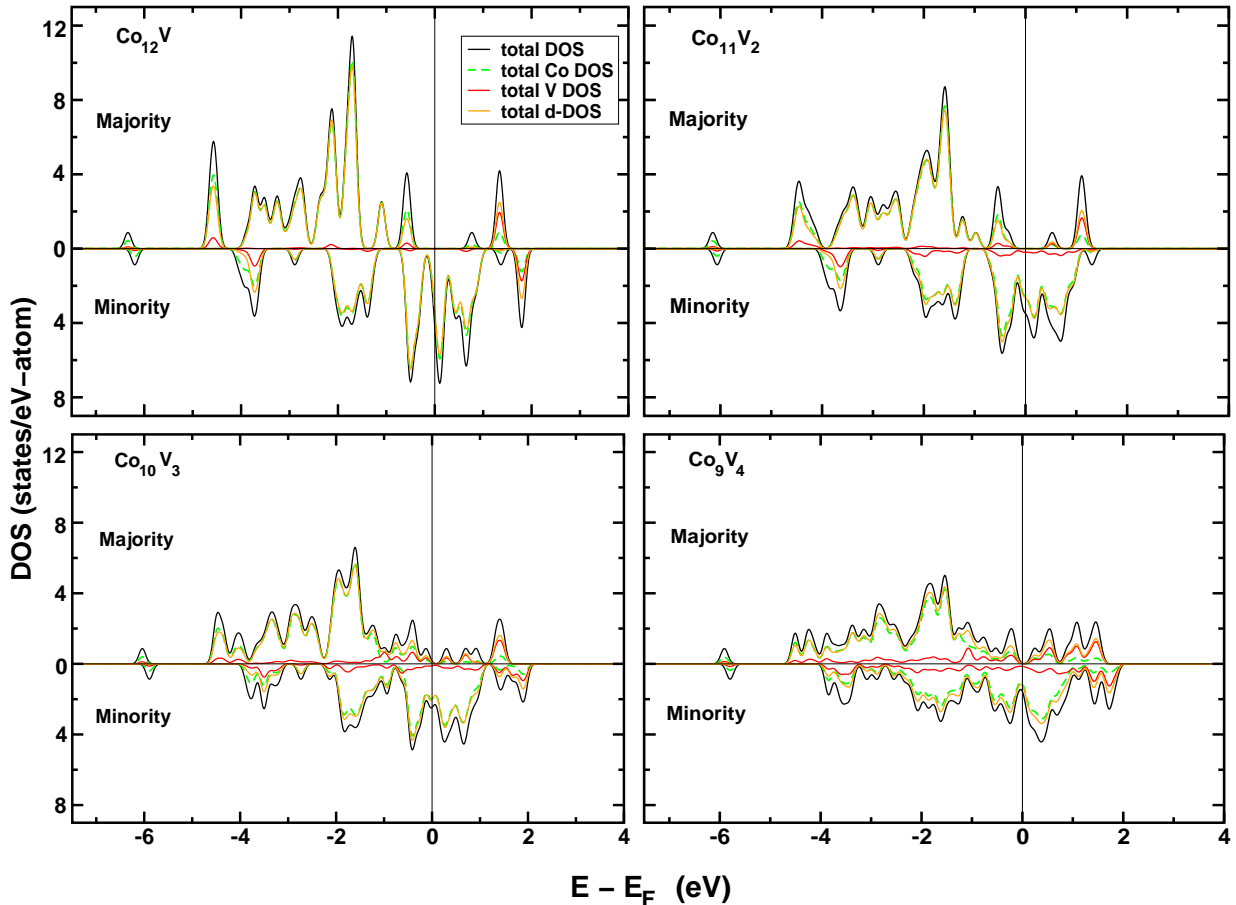


FIG. 6: (Color online) Total DOS per atom, Co projected DOS per atom, V projected DOS per atom and total d-projected DOS per atom for the optimal structures of  $\text{Co}_{12}\text{V}$ ,  $\text{Co}_{11}\text{V}_2$ ,  $\text{Co}_{10}\text{V}_3$  and  $\text{Co}_9\text{V}_4$ . The smearing width is fixed at 0.1 eV. Vertical line through zero is the Fermi energy ( $E_F$ ).

early transition metal substrate and the exterior twelve Co atoms correspond to a late transition-metal monolayer.

In order to see the chemical activity of the central V-atom, we have plotted in Fig. 7, the projected total DOS of the central V-atom for each of the  $\text{Co}_{13-m}\text{V}_m$  clusters. First of all, it is seen that there is no finite states at the Fermi energy, meaning that the central V-atom is not chemically active. Also each of the majority and minority spin channels has two large peaks: one is deep below the Fermi energy and another is above the Fermi energy. However, the peak heights gradually decrease, the states are broadened out and shifted towards higher energy with increasing V-concentrations. It is therefore indicating that the presence of surface V-atoms induces some sort of chemical activeness to the central atom.

## V. CHEMISORPTION WITH $\text{H}_2$ MOLECULES

In order to gain some understanding about the cluster chemical reactivity, we have investigated the chemisorbed structures of the  $\text{Co}_{13-m}\text{V}_m$  clusters upon  $\text{H}_2$  adsorption. To check the robustness of our chemisorption calculations involving H-atoms, we have first calculated the cohesive energy, bond length and vibrational frequency of  $\text{H}_2$  dimer. Our calculated values have been listed in Table IV. These values are typical for gradient-corrected calculations of  $\text{H}_2$ , which have been done before<sup>40</sup> and they agreed reasonably well with experiment.<sup>41</sup>

We have then performed an exhaustive search for the MES, taking  $\text{H}_2$  at different possible places on the MES of the corresponding bare cluster for each composition. Fig. 8 shows our calculated lowest energy chemisorption structures after  $\text{H}_2$  adsorption for clusters of all compositions. First thing to notice is that  $\text{H}_2$  molecule chemisorbs dissociatively in each case, *i.e.* the distance between the two H-atoms in the chemisorption structures is much larger

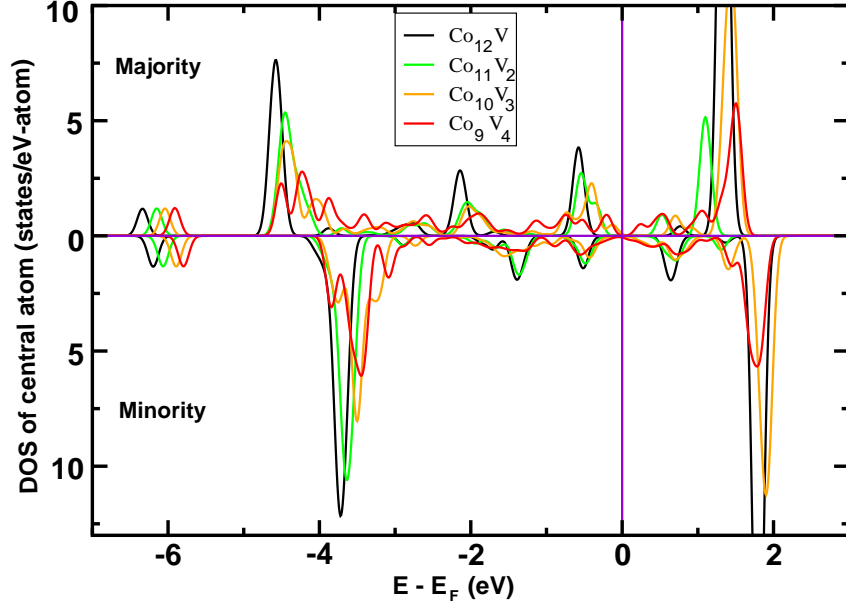


FIG. 7: (Color online) Total DOS of the central V atom in the optimal structures of  $\text{Co}_{12}\text{V}$ ,  $\text{Co}_{11}\text{V}_2$ ,  $\text{Co}_{10}\text{V}_3$  and  $\text{Co}_9\text{V}_4$ . The Fermi energy ( $E_F$ ) is fixed at zero.

TABLE IV: Theoretical values of cohesive energy, bond length and vibrational frequency for  $\text{H}_2$  dimer in the present calculation. Experimental values in Ref. 41 are also given for comparison.

	Cohesive energy (eV)	Bond length ( $\text{\AA}$ )	Vibrational frequency ( $\text{cm}^{-1}$ )
Theory	4.520	0.752	4339
Experiment	4.750	0.741	4395

than the H-H bond length of an isolated  $\text{H}_2$  molecule. The chemisorption gives rise to moderate perturbation to the structures and makes them more symmetric (*i.e.* surface bonds are now less dispersive) compared to the parent structure without hydrogen. There are three possible ways for the H-atoms to be adsorbed on each cluster : on top of an atom (one fold), at a bridge position between two atoms (two fold) and at the hollow site of a triangular plane on the cluster (three fold). Again, as the surface contains two species of atoms for  $\text{Co}_{11}\text{V}_2$ ,  $\text{Co}_{10}\text{V}_3$  and  $\text{Co}_9\text{V}_4$ , then the one fold position can be on top of a surface V-atom or on top of a surface Co-atom. Two fold position can be the top of a V-V bond, Co-V bond or a Co-Co bond which can be nearer to or away from the V-site. Similarly, in triangular plane, there are several possibilities : (i) all the three atoms can be V-atoms (only possible for  $\text{Co}_9\text{V}_4$ ), (ii) one Co atom and two V-atoms,

(iii) two Co-atoms and one V-atom, and (iv) all three are Co-atoms. We have considered all these possible combinations during optimization. It is, however, seen that in each of the optimized structures, H-atoms adsorb at the hollow site on the surface and for  $m \geq 2$ , they prefer the association of the local V atom. For example in the  $\text{Co}_9\text{V}_4\text{H}_2$  cluster, one H-atom adsorbs at the hollow site of V-V-V triangular plane and the other H atom on top of a V-V-Co triangular plane. For  $\text{Co}_{11}\text{V}_2\text{H}_2$ , the H-atoms appear to adsorb at the bridge positions, but they are inclined with an angle such that the absorption tends toward a three fold configuration. The preference of more coordinated hollow site is likely due to geometric arrangements. It allows the H-atom to interact more with the V or Co atoms. On the other hand, the V-site preference of H-atom is due to the formation of stronger *s-d* bond with V-atom compared to that with Co-atom.

The higher reactivity of the  $\text{Co}_{13}$  cluster compared to the  $\text{Co}_{12}\text{V}$  cluster, while both of them have the same twelve Co-atoms on the surface, can be understood from charge transfer analysis. We have computed the charge enclosed within a sphere around each surface atom of the optimal structures of  $\text{Co}_{13}\text{H}_2$  and  $\text{Co}_{12}\text{VH}_2$  clusters. It is seen that the amount of charge on each surface Co-atoms in the  $\text{Co}_{13}\text{H}_2$  cluster is larger by about 0.2 (in unit of electronic charge) than that of  $\text{Co}_{12}\text{VH}_2$  and it is mainly contributed by the *d*-electrons of surface Co atoms. Therefore stronger *3d-1s* interaction between surface Co-atoms and chemisorbed H-atoms in case of  $\text{Co}_{13}\text{H}_2$  increases its reactivity. This result is in accor-



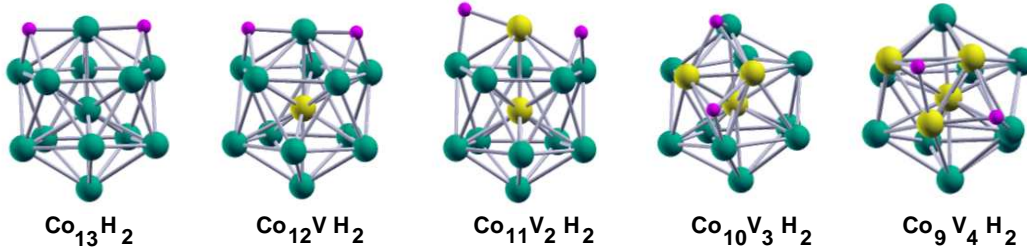


FIG. 8: (Color online) The calculated minimum energy chemisorption structures with  $H_2$  on the minimum energy structures of  $Co_{13-m}V_m$  ( $m = 0-4$ ). It is clearly seen that hollow site on the surface is preferred by chemisorbed hydrogen. Color convention is same as in Fig. 2 with pink colored dots representing H atom.

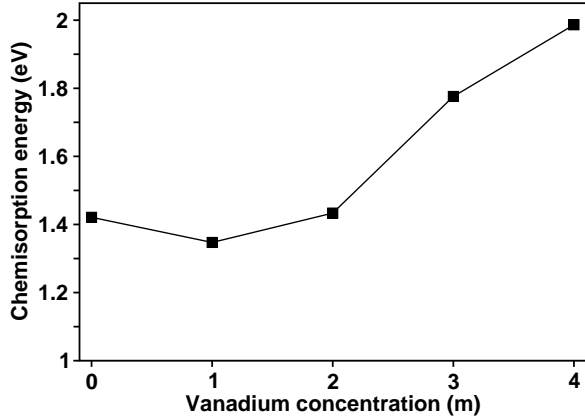


FIG. 9: The calculated chemisorption energy (using Eqn. 4) for  $Co_{13-m}V_mH_2$  clusters.

dance with that of Fujima *et al*<sup>42</sup> who also predicted the stronger interaction between  $1s$  of H atom and the  $3d$  orbital of the surface Co atom in the  $Co_{13}H_2$  cluster compared to that in the  $Co_{12}VH_2$  cluster using density of state analysis. They showed that the anti-bonding orbital component between the H- $1s$  electron and the  $3d$  electron of the surface Co-atoms shifts further away above the HOMO in case of  $Co_{13}H_2$  compared to that of  $Co_{12}VH_2$ , while the bonding orbital components for both the clusters stay almost at the same energy position below the HOMO. Extending the charge transfer analysis for the  $Co_{13-m}V_mH_2$  clusters with  $m = 2, 3$  and 4, we find that the average charge per surface V-atom is gradually increasing with the increase of V-concentration which indicates the formation of stronger V-H bonds at the surface with increasing V-doping. Average charge per surface Co-atom for these three clusters, however, remains almost the same.

Fig. 9 shows the plot of chemisorption energy with increasing V-concentration, where the chemisorption en-

ergy is defined as

$$D_e(E) = E(Co_{13-m}V_m) + E(H_2) - E(Co_{13-m}V_mH_2) \quad (4)$$

It is a positive quantity and gives a measure of binding strength of  $H_2$  molecule with the cluster. The plot shows a minimum for  $Co_{12}VH_2$  again indicating the lowest binding efficiency of  $Co_{12}V$  with H. However, chemisorption energy increases with increasing V concentration. The source of this chemisorption energy is the cluster rearrangement energy (*i.e* the energy change due to the geometrical rearrangement of the cluster upon chemisorption) and the efficient cluster-adsorbate bonding in presence of V due to more efficient  $s-d$  hybridization.

## VI. SUMMARY AND CONCLUSIONS

To summarize, we have studied the geometric and electronic structures of V doped  $Co_{13}$  clusters and their chemisorption towards hydrogen molecules using first principles density functional calculation. The lowest energy structures of all compositions prefer to have icosahedral geometry, unlike hexagonal symmetry preference of the pure Co clusters. For the  $Co_{12}V$  cluster, the single V atom prefers to sit at the central site, thereby guarded by all the surface Co atoms and cannot participate directly in the chemisorption reaction. Consequently reactivity of  $Co_{12}V$  becomes very less. On the other hand, for more than one V atom doping, the additional V-atoms reside on the surface and come in direct contact with chemisorbed H-atom and reactivity increases. Our calculated spin gaps, density of states and charge transfer analysis explain nicely the stability of clusters and their tendency towards chemisorption. In the chemisorbed structures, H-atoms adsorb dissociatively at the more coordinated hollow sites and they prefer V-site association due to stronger  $3d-1s$  hybridization. To have better insight into the chemisorption reaction, one needs to study the transition states for the optimal cluster of each composition and we believe that calculation of activation barriers will also lead to same conclusion as we have predicted

here.

### Acknowledgments

S. D. is thankful to Council of Scientific and Industrial Research (Government of India) for financial sup-

port. T.S.D. thanks Department of Science and Technology, India for Swarnajayanti fellowship and the support through Advanced Materials Research Unit.

- <sup>1</sup> R. Ferrando, J. Jellinek, and R. L. Johnston, *Chem. Rev.* **108**, 845 (2008).
- <sup>2</sup> J. Bansmann, S. H. Baker, C. Binns, J. A. Blackman, J. -P. Bucher, J. Dorantes-Davila, V. Dupuis, L. Favre, D. Kechrakos, A. Kleibert, K. -H. Meiwes-Broer, G. M. Pastor, A. Perez, O. Toulemonde, K. N. Trohidou, J. Tuailleon, and Y. Xie, *Surf. Sci. Rep.* **56**, 189 (2005).
- <sup>3</sup> J. H. Sinfelt, *Bimetallic Catalysts : Discoveries, Concepts and Allpications*, J. Wiley, New York, 1983.
- <sup>4</sup> N. Tushima, T. Yonezawa, *New J. Chem.* **22**, 1179 (1998).
- <sup>5</sup> A. V. Ruban, H. A. Skriver, J. K. Norskov, *Phys. Rev. B* **59**, 15990 (1999).
- <sup>6</sup> G. Bozzolo, J. Ferrante, R. D. Noebe, B. Good, F. S. Honey, P. Abel, *Comput. Matter. Sci.* **15**, 169 (1999).
- <sup>7</sup> F. Besenbacher, I. Chorkendorff, B. S. Clausen, B. Hammer, A. M. Molenbroek, J. K. Norskov, I. Stensgaard, *Science* **279**, 1913 (1998).
- <sup>8</sup> A. M. Molenbroek, S. Haukka, B. S. Clausen, *J. Phys. Chem. B* **102**, 10680 (1998).
- <sup>9</sup> A. Bongiorno and U. landman, *Phys. Rev. Lett.* **95**, 106102 (2005).
- <sup>10</sup> E. Kaxiras, *Phys. Rev. Lett.* **64**, 551 (1990).
- <sup>11</sup> G. H. Guvelioglu, P. Ma, X. He, R. C. Forrey and H. Cheng, *Phys. Rev. Lett.* **94**, 026103 (2005); Y. Jinlong, X. Chuanyun, X. Shangda and W. Kelin, *Phys. Rev. B* **48**, 12155 (1993); R. Q. Zhang, T. S. Chu, H. F. Cheung, N. Wang and S. T. Lee, *Phys. Rev. B* **64**, 113304 (2001); J. Gavnholt and J. Schiotz, *Phys. Rev. B* **77**, 035404 (2008); D. R. Alfonso, S.-Y. Wu, C. S. Jayanthi, E. Kaxiras, *Phys. Rev. B* **59**, 7745 (1999); S. K. Nayak, S. E. Weber, P. Jena, K. Wildberger, R. Zeller, P. H. Dederichs, V. S. Stepanyuk and W. Hergert, *Phys. Rev. B* **56**, 8849 (1997); H. Kawamura, V. Kumar and Y. Kawazoe, *Phys. Rev. B* **70**, 193402 (2004).
- <sup>12</sup> R. L. Whetten, D. M. Cox, D. j. Trevor and A. Kaldor, *Phys. Rev. Lett.* **54**, 1494 (1985); L. Holmgren, H. Gronbeck, M. Andersson and A. Rosen, *Phys. Rev. B* **53**, 16644 (1996).
- <sup>13</sup> S. Nonose, Y. Sone, K. Onodera, S. Sudo and K. Kaya, *J. Phys. Chem.* **94**, 2744 (1990).
- <sup>14</sup> G. C. Bond, *Heterogeneous Catalysis*, 2nd Ed.; Clarendon Press: Oxford, 1987.
- <sup>15</sup> A. Nakajima, T. Kishi, T. Sugioka, Y. Sone and K. Kaya, *J. Phys. Chem.* **95**, 6833 (1991).
- <sup>16</sup> A. Pramann, K. Koyasu and A. Nakajima, *J. Phys. Chem. A* **106**, 2483 (2002).
- <sup>17</sup> R. L. Whetten, D. M. Cox, D. J. Trevor and A. Koldor, *Phys. Rev. Lett.* **54**, 1494 (1985).
- <sup>18</sup> K. Hoshino, T. Naganuma, K. Watanabe, Y. Konishi, A. Nakajima, K. Kaya, *Chem. Phys. Lett.* **239**, 369 (1995).
- <sup>19</sup> Vienna *ab initio* simulation package (VASP), Technische Universität Wien, 1999; G. Kresse and J. Hafner, *Phys. Rev. B* **47**, 558 (1993); G. Kresse and J. Furthmuller, *Phys. Rev. B* **54**, 11169 (1996).
- <sup>20</sup> P. E. Blöchl, *Phys. Rev. B* **50**, 17953 (1994).
- <sup>21</sup> G. Kresse and D. Joubert, *Phys. Rev. B* **59**, 1758 (1999).
- <sup>22</sup> J. P. Perdew, K. Burke and M. Ernzerhof, *Phys. Rev. Lett.* **77**, 3865 (1996).
- <sup>23</sup> M. C. Payne, M. P. Teter, D. C. Allan, T. A. Arias and J. D. Joannopoulos, *Rev. Mod. Phys.* **64**, 1045 (1992).
- <sup>24</sup> S. Datta, M. Kabir, S. Ganguly, B. Sanyal, T. Saha-Dasgupta and A. Mookerjee, *Phys. Rev. B*, **76**, 014429 (2007).
- <sup>25</sup> *Theory of Atomic and Molecular Clusters*; Ed. J. Jellinek, Springer, Berlin, p. 277 (1999) and references therein.
- <sup>26</sup> J. Jellinek, E. B. Krissinel, *Chem. Phys. Lett.* **258**, 283 (1996); J. Jellinek, E. B. Krissinel, *Chem. Phys. Lett.* **272**, 301 (1997).
- <sup>27</sup> J. Alonso, *Chem. Rev.* **100**, 637 (2000).
- <sup>28</sup> Mukul Kabir, D. G. Kanhere and Abhijit Mookerjee, *Phys. Rev. B* **73**, 224443 (2006); T. M. Briere, M. H. F. Sluiter, V. Kumar and Y. Kawazoe, *Phys. Rev. B* **66**, 064412 (2002).
- <sup>29</sup> O. Dieguez, M. M. G. Alemany, C. Rey, P. Ordejon and L. J. Gallego, *Phys. Rev. B* **63**, 205407 (2001).
- <sup>30</sup> E. K. Parks, L. Zhu, J. Ho and S. J. Riley, *J. Chem. Phys.* **102**, 7377 (1995); N. N. Lathiotakis, A. N. Andriotis, M. Menon and J. Connolly, *J. Chem. Phys.* **104**, 992 (1996).
- <sup>31</sup> S. Datta, M. Kabir, T. Saha-Dasgupta, and A. Mookerjee; to be published.
- <sup>32</sup> S. Datta, Ph. D Thesis, S. N. Bose National Centre for Basic Sciences (2008).
- <sup>33</sup> X. Xu, S. Yin, R. Moro and W. A. de Heer, *Phys. Rev. Lett.* **95**, 237209 (2005).
- <sup>34</sup> S. Ganguly, M. Kabir, S. Datta, B. Sanyal and A. Mookerjee, *Phys. Rev. B* **78**, 014402 (2008).
- <sup>35</sup> A. Kant, B. Strauss, *J. Chem. Phys.* **41**, 3806 (1964).
- <sup>36</sup> S. P. Walch, C. W. Bauschlicher Jr., B. O. Roos and C. J. Nelin, *Chem. Phys. Lett.* **103**, 175 (1983).
- <sup>37</sup> C.-X. Su, D. A. Hales and P. B. Amentrout, *J. Chem. Phys.* **99**, 6613 (1993).
- <sup>38</sup> M. El-Batanouny, M. Stronger, G. P. Williams and J. Colbert, *Phys. Rev. Lett.* **46**, 269 (1981).
- <sup>39</sup> M. V. Ruckman and M. Strongin, *Phys. Rev. B* **29**, 7105 (1984); D. Prigge, W. Schlerk and E. Bauer, *Surf. Sci. Lett.* **123**, L698 (1982).
- <sup>40</sup> G. Kresse and J. Hafner, *Surf. Sc.* **459**, 287 (2000).
- <sup>41</sup> K. P. Huber and G. Hertzberg, *Molecular Structure and Molecular Spectra IV: Constants of Diatomic Molecules* (Van Norstrand Reinhold, New York, 1979).
- <sup>42</sup> N. Fujima and T. Yamaguchi, *J. Phys. Society of Japan* **61**, 1724 (1992).